Exploring the conformational dynamics and membrane interactions of PorB from C. glutamicum: A multi-scale molecular dynamics simulation study

ARTICLE *in* BIOCHIMICA ET BIOPHYSICA ACTA · FEBRUARY 2011

Impact Factor: 4.66 · DOI: 10.1016/j.bbamem.2011.02.015 · Source: PubMed

3 AUTHORS:

Ángel Piñeiro
University of Santiago de Compostela
54 PUBLICATIONS **1,037** CITATIONS
SEE PROFILE

Peter J Bond
University of Cambridge
82 PUBLICATIONS **2,341** CITATIONS
SEE PROFILE

Syma Khalid
University of Southampton
80 PUBLICATIONS **1,216** CITATIONS
SEE PROFILE

Biochimica et Biophysica Acta 1808 (2011) 1746–1752

Contents lists available at ScienceDirect

Biochimica et Biophysica Acta

journal homepage: www.elsevier.com/locate/bbamem

Exploring the conformational dynamics and membrane interactions of PorB from *C. glutamicum:* A multi-scale molecular dynamics simulation study

Ángel Piñeiro [a,c], Peter J. Bond [b], Syma Khalid [c,*]

[a] Soft Matter and Molecular Biophysics Group, Department of Applied Physics University of Santiago de Compostela, Campus Vida, 15782, Santiago de Compostela, Spain
[b] The Unilever Centre for Molecular Science Informatics, Department of Chemistry, Lensfield Road, University of Cambridge, Cambridge, CB2 1EW, UK
[c] School of Chemistry, University of Southampton, Highfield, Southampton SO17 1BJ, UK

ARTICLE INFO

Article history:
Received 17 December 2010
Received in revised form 17 February 2011
Accepted 18 February 2011
Available online 24 February 2011

Keywords:
Outer membrane protein
Porin
Molecular dynamics
Coarse-grained
Multiscale
C. glutamicum

ABSTRACT

Members of the gram-positive *mycolata* bacteria have unusual cell envelopes which help them to avoid the immune system and the effects of most antibiotics, whilst rendering them permeable to solutes of importance in industrial bioconversion. It is therefore of interest to understand the molecular mechanisms for this selective permeability. PorB is an unusual porin from the outer membrane (OM) of *Corynebacterium glutamicum*. It has been proposed as an atypical α-helical, symmetrical homo-pentameric architecture, with an unusual distribution of polar amino acids on its surface. The proposed structure is too short to traverse a typical phospholipid bilayer, in contrast with the β-barrel porins of Gram-negative bacteria. Nevertheless, it has been shown to form small anion-selective channels in membranes typical of *Escherichia coli*. To further understand its function, we have performed ~400 ns of all-atom and ~270 μs of coarse-grained simulations of PorB in a range of membrane mimetic and phospholipid milieus. Our results suggest that PorB can undergo spontaneous conformational rearrangements that allow it to adapt to its local lipid environment. We speculate that the increased flexibility of this α-helical porin in comparison with rigid β-barrels may be an adaptation for the heterogeneous mycolic OM, and explains its demonstrated ability to form measurable pores with phospholipid membranes.

1. Introduction

The outer membranes (OMs) of gram negative bacteria are composed of phospholipids and lipopolysaccharides. They are rendered selectively permeable by transmembrane channel proteins called porins, whose structures have been extensively characterized and are typically based on a β-barrel architecture [1–3]. In contrast, members of the gram positive *mycolata* taxon, including *Mycobacteria* and *Corynebacteria*, share a less well-characterized OM, rich in mycolic acid whose acyl tail length varies between species [4]. Many of these bacteria are the causative agents of a variety of serious diseases in mammals (including tuberculosis and diphtheria), aided by their characteristic cell walls, which render them resistant to most antibiotics and help them to evade the immune system. In addition, some non-pathogenic *Corynebacteria,* such as *Corynebacterium glutamicum*, are employed for industrial applications including amino acid production, bioconversion of steroids and hydrocarbon degradation [5]. It is therefore crucial to understand the nature of the outer cellular envelope, and in particular, how it is rendered selectively permeable to solutes and ions.

Clues to the molecular mechanisms of permeability may be provided by a structural knowledge of the membrane associated protein machinery. The first available high-resolution structure of an outer membrane protein (OMP) from the *mycolata* bacterial group was that of the main porin from *Mycobacterium smegmatis*, MspA. X-ray analysis revealed a ~10 nm long, homooctameric, goblet-like conformation containing two consecutive β-barrels, unlike the structure of any gram negative bacterial porin solved to date. This unusual architecture likely reflects structural adaptations particular to the ~7–8 nm, mycobacterial mycolic acid layer [6]. More recently, an equally unusual X-ray structure of the repeating subunit from the oligomeric porin PorB of *C. glutamicum* was solved [7]. It is one of four porin proteins identified to date within this species, the major cell wall being formed by a heterooligomer of PorA and PorH [8]. PorB is unusual in that it lacks the β-barrel architecture typical of gram-negative OM porins. Ziegler et al. reported sixteen independent X-ray structures of the PorB monomer, in four different crystal forms. All of the sixteen structures revealed the same tightly packed core, consisting of 70 residues forming four α-helices held together by a disulfide bridge, with more variable 17 and 12 residue long N- and C-terminal extensions, but with no obvious translocation channel (Fig. 1). The difficulties in obtaining an X-ray structure of the functional channel may in part be due to working isolated PorB. In

* Corresponding author. Tel.: +44 2380 59476; fax: +44 2380 3781.
E-mail addresses: Angel.Pineiro@usc.es (Á. Piñeiro), pjb91@cam.ac.uk (P.J. Bond), S.Khalid@soton.ac.uk (S. Khalid).

0005-2736/$ – see front matter © 2011 Elsevier B.V. All rights reserved.
doi:10.1016/j.bbamem.2011.02.015

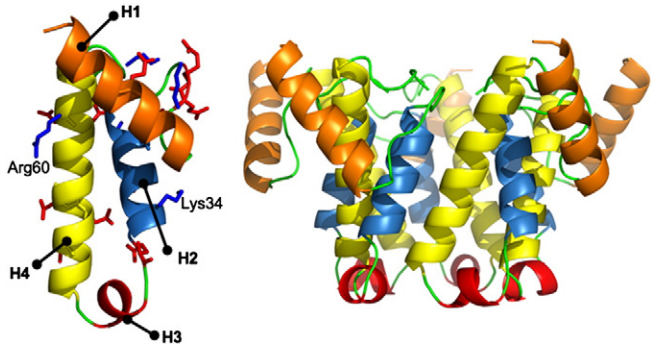

Fig. 1. PorB subunit (left) and the pentameric model (right) structure proposed by Ziegler et al. [7]. In the monomeric structure the acid and basic residues are colored in red and light blue, respectively. The basic residues Arg60 and Lys34 pointing toward the hydrophobic side of the protein as well as helices H1–H4 (in orange, blue, red and yellow, respectively) are labeled.

C. glutamicum, PorB is expressed together with a closely related protein PorC, which may play a key role in the formation of the anion-selective cell wall channel [7]. PorB has been shown to form small anion-selective channels with an average single-channel conductance of about 0.7 nS in 1 M KCl in black lipid membranes [9,10]. Based on this, and on the structure of the monomeric core, a pentameric model of the functional porin was constructed (Fig. 1). The model was based on the assumption of symmetry around a five-fold axis along which the pore would lie, with most polar amino acid sidechains pointing into the interior of the porin.

Nevertheless, a number of questions remain concerning the structure of *Corynebacterial* porins. As well as containing a high percentage of α-helical structure, PorB is shorter than other porins; at less than 3.5 nm in length, it would not fully traverse a typical phospholipid bilayer. Similar to MspA, its atypical architecture may reflect the difference in its natural membrane environment compared to that of Gram-negative species. Whilst the exact composition and architecture of the OM of *C. glutamicum* is unknown, recent studies of the *Corynebacterial* cell wall suggest that its OM is thinner than in Gram-negative bacteria, with an estimated width of ~4–5 nm [6]. The hydrophobic patch on the outer surface of MspA has been estimated to be ~7.1 nm [11]. On the other hand, single-channel measurements were performed in a bilayer composed of phospholipids more typical of e.g. *E. coli* cells, hinting that the protein may be able to insert into different membrane environments, whilst still retaining its function. This is intriguing, given the atypical distribution of amino acids over the surface of the protein. Porins, and membrane proteins in general, normally feature a largely hydrophobic outer surface, specialized for interaction with the central acyl chain region of a phospholipid bilayer, framed on either side by tryptophan/tyrosine and/or polar residues which serve to anchor the protein to the membrane/water interfacial region [12]. In contrast, PorB features a hydrophobic patch at the cell-facing mouth of the porin formed by phe38 and trp39 in H3 helices (Fig. 1, in red), and contains a number of polar and charged residues (including one lysine, arginine, and aspartate) per monomer whose sidechains would likely be exposed to the acyl chains region of a typical lipid bilayer. Such exposure would be expected to present a high energetic cost to the transmembrane insertion of PorB [13].

To further understand how PorB may form permeable pores within different membrane environments, we present results from a combination of atomistic and coarse-grained (CG) molecular dynamics (MD) simulations. These have been employed to study the conformational dynamics of the monomer and pentamer in a variety of membrane mimetic systems. Our results suggest that the PorB pentamer can undergo spontaneous conformational changes that allow it to adjust to the local lipid environment. We identify a conformation that is particularly well-suited to a phospholipid environment.

2. Methods

2.1. Atomistic simulations

2.1.1. Simulation systems

Simulations of the PorB monomer (PDB ID: 2VQG) were performed at the water/air and at the water/hexane interfaces in order to investigate its stability and conformational dynamics. The setup details of both sets of simulations are provided in the supplementary information. Briefly, each simulation system was built by placing the PorB monomer in a hexagonal prism shaped box with its symmetry axis in the *z* direction and the H4 and H2 helix axes (Fig. 2) parallel to the *xy* plane. The water/hexane interface system consisted of ~12,000 water molecules, 6 Na^+ ions (to yield a charge neutral system at physiological pH), one protein subunit, and ~1,300 hexane molecules. Simulations of the pentamers were setup by introducing the PorB model (coordinates for the original model were kindly provided by Georg Schulz) and bound Ca^{2+} cations into the center of a hexagonal prism shaped box with the symmetry axes of the protein and the box parallel to the *z* direction. The final systems consisted of ~14,000 water and ~200 lipid molecules in addition to the 15 Ca^{2+} ions and 5 protein subunits. Sequential equilibration stages in which the strength of the artificial restrictions on the system were gradually reduced were performed such that the total equilibration time was 22 ns. Further details of the system setup and equilibration protocol are provided in the supplementary information.

2.1.2. Simulation protocols

MD simulations were performed by applying the recently published half-ε double-pairlist method [14] to ensure compatibility of the Berger united atom parameters [15,16] used for the lipids with the OPLS-AA force field [17,18] employed for the protein and ions. Simple point charge (SPC) water molecules [19] were included to solvate the systems. All the simulations were performed using periodic boundary conditions in the three spatial dimensions with hexagonal prism shaped boxes. For the simulations in lipid bilayers a semi-isotropic Parrinello–Rahman barostat [20,21] was employed to maintain the pressure independently in the *xy* plane and in the *z* direction at 1 bar with a coupling constant of 2 ps. The isothermal compressibility constant was 4.5×10^{-5} bar^{-1}. The same protocol was employed for the simulations at the water/hexane interfaces for the *z* dimension, while the position of the box walls perpendicular to the *xy* plane was fixed. The simulations at the water/air interface were performed at constant volume. In all the simulations the temperature

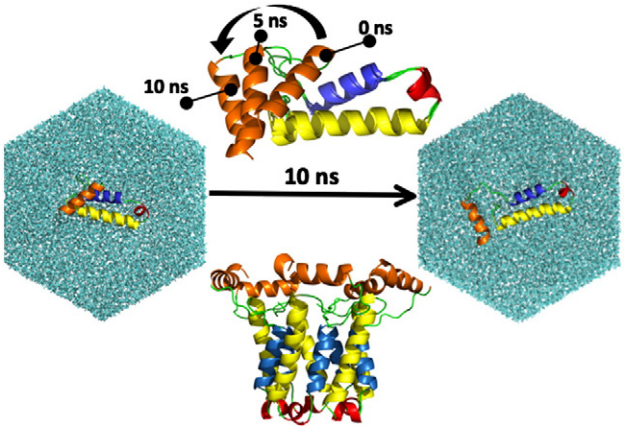

Fig. 2. Initial (left) and final (right) conformations of a porB subunit -original structure at the water/hexane interface. For clarity, hexane molecules are not shown while waters are represented in cyan sticks. Alignment of the H2–H4 protein conformations at 0, 5 and 10 ns (top) and a side view of the modified pentameric model (bottom) built using the final conformation of the monomer simulation at the water/hexane interface, with helices H1–H4 in orange, blue, red and yellow respectively.

was kept constant using a Nosé–Hoover thermostat [22,23] by coupling the lipids or hexane molecules, the protein and the solvent (water and ions) groups independently with a common period of 0.1 ps. The simulations in the lipid bilayer were performed at 310 K while the simulations at the water/air and water/hexane were performed at 298 K. A cutoff of 1.2 nm was employed for the Lennard–Jones potential. The long range interactions were calculated using the particle mesh Ewald method [24,25] with a 1.2 nm real space cutoff and a 0.15 nm space grid. For the simulations at the water/air interface, with slab geometry, the Ewald sum in three dimensions with a correction term (EW3DC) [26] was used to avoid artifacts due to interactions between replicas in the *z* dimension. The equations of motion were integrated using the leapfrog method [27] with a 2 fs time step. The bonds lengths and water angle were constrained using the SETTLE algorithm [28] while the LINCS algorithm [29] was used to constrain bond lengths in the protein, hexane and lipid molecules. All the simulations were performed using the GROMACS package [30–33] version 4.0.5. By means of the scripted protocols, three independent replicas of each simulation were performed under equivalent conditions.

2.2. Coarse-grained simulations

2.2.1. Simulation systems

Simulations of the pentameric models were performed by introducing the CG PorB models into the center of a hexagonal prism shaped simulation box of size $15\times15\times20$ nm. Two hundred randomly orientated CG POPC and/or DLPC molecules were added at random locations inside the simulation box taking care to avoid overlaps with the protein. Five POPC concentrations (0%, 25%, 50%, 75% and 100%) were employed. Following the addition of lipids, 10,000 CG water particles (corresponding to 40,000 real water molecules) and 30 Na + counter-ions were added to the simulation box. The resulting system was simulated for 5 μs and five replicas of each simulation were performed. Positional restraints were used to immobilise the protein thus enabling the bilayer to form around it from an initially random arrangement of lipids and water around the protein. No restrictions other than those imposed by the CG force field were applied for the ions, lipids and waters. Five replicas were performed for each concentration and model protein using different initial random configurations of the molecules.

2.2.2. Simulation protocols

The CG parameters developed by Marrink [34] were employed to model all the lipid molecules in the system, with protein parameters developed by Bond [35]. In this approach, approximately four heavy (i.e. not H) atoms are represented by a single particle. The protein topology was generated as in [36,37]. As in the case of the atomistic simulations, all the CG simulations were performed using the GROMACS 4.0.5 simulation package. The neighbor list was updated every 10 steps. All simulations were performed at constant temperature, pressure and number of particles. The temperatures of the protein, lipids and solvent were coupled separately using the Berendsen thermostat at 323 K, with a coupling constant of 10 ps [38]. The system pressure was anisotropically coupled using the Berendsen barostat at 1 bar with a coupling constant of 10 ps and a compressibility of 5×10^{-6} bar K^{-1}. The integration time step was 30 ps.

3. Results

3.1. Spontaneous conformational changes in the PorB monomer

To evaluate the stability and orientation of the PorB monomer and to relieve any effects of crystal packing in the X-ray structure, we first simulated the monomer in a water/membrane mimetic environment. The PorB monomer was simulated at a water/hexane interface to explore its conformational stability. The water/hexane interface provides a simplified model of a solvated lipid bilayer. The atomistic details of individual lipids are omitted, but the hydrophobic/polar nature of the environment is captured. As the conformational landscape of such an environment is smoother than more complex conformational landscape of lipid bilayers, conformational rearrangements are expected to be observed on much shorter timescales, thus we employed these models to enable the monomer to relax in an environment that mimics a solvated lipid bilayer. (see details in the Supplementary Information). During each simulation (three replicas were performed for improved sampling), the monomers remained stable at the water surface with H2 and H4 lying parallel to the interfacial plane. Whilst the overall secondary structure was maintained, H1 was observed to pivot around the Cys5–Cys64 disulphide bridge. The spontaneous rotation of H1 was reproducible in the three replicas performed under the same conditions. The angle between the axes of H1 and H4 increased from ~50° to ~100° after 10 ns of MD simulation. Moreover, the Lys34 and Arg60 sidechains, which were initially in contact with the hydrophobic solvent, adjusted toward the polar phase. The final conformation of the monomer was aligned to each of the five subunits of the original model to produce a modified model of pentameric PorB (Fig. 2). In order to optimize the interactions between side chains, a long equilibration protocol with decreasing strength on the positional restraints imposed on the protein structure was performed: all the heavy atoms of the pentamer were restrained using a force constant of 1000 kJ mol^{-1} nm^{-2}; this was reduced in decrements of 200 kJ mol^{-1} nm^{-2} until a final equilibrated model devoid of any steric, clashes of sidechains was achieved.

3.2. Stability of the PorB pentamer in a phospholipid environment

To examine the likely conformation of the PorB pentamer in phospholipids, a total of 90 ns of atomistic simulation time of the original model (proposed by Ziegler et al.) was computed, split into three trajectories to diversify the exploration of conformational space and hence improve sampling. Similarly, 90 ns of simulation time was computed for a modified model of PorB, based on simulations of the monomer, in which helix H1 had reoriented relative to the initial model. Both models were stable on the timescale of the simulations, exhibiting minimal loss of secondary structure (Supplementary Information). The root mean squared deviation (RMSD) of the protein backbone of each subunit relative to the respective initial model was ~0.1–0.2 nm for each system (Supplementary Information). Such conformational drift over these simulation timescales is comparable to that of other β-barrel, bacterial OMPs [39,40]. The high stability of the pentameric bundle was observed to be due to the presence of 15 Ca^{2+} ions, which remained bound to carboxylate groups of acidic residues within the pore throughout each simulation, and served to cross-link the internal bundle composed of helices H1, H2, and H3. This is reflected in the stable RMSD calculated for these helices only (Supplementary Information). We performed an additional set of 3 simulations for each model in which the simulation systems were neutralized by placing 30× Na^{+} in the bulk solvent. The RMSD of the protein backbone was much higher (4–5 Å compared to only 1–2 Å in the presence of Ca^{2+} ions in the pore, within 14 ns) in all simulations. Visual inspection of the snapshots revealed that the protein structure is more deformed after 14 ns in the absence of Ca^{2+} ions within the pore. This suggests the ions within the pore play a crucial role in maintaining the structural integrity of the pentamer. Comparison of the original and modified models of the pentamer revealed the primary differences concerned helix H1. Whilst H1 in the original model exhibited minimal structural drift (RMSD ~0.1 nm), that of the modified model was higher with an RMSD up to ~0.2 nm. This resulted from the ability of this helix in the modified model to adapt to

the membrane/water interface. The root mean square fluctuations of the residues in H1 were also higher in the modified model compared to the original model (Supplementary Information). The RMSD of the residues located at the interface between protein subunits for the modified model is ~0.15 nm.

Analysis of the pore radius profile of each model revealed a constriction formed by the Arg25 residues pointing into the lumen of the pore (Supplementary Information). The constriction was initially narrower in the modified model (radius of 0.15 nm compared to 0.31 nm in the original model). However, during the course of the simulations, the pore in both models converged to similar dimensions. Encouragingly, based on the mean pore dimensions, and assuming that the pores were filled with an electrolytic solution of reduced ionic mobility [41], we estimated that both models should have a conductance of 0.4–0.5 nS in 1 M KCl, which is reasonably close to the experimentally measured conductance of 0.7 nS, within the limits of error.

During simulations of the original model, the polar headgroups of several lipid molecules (and accompanying water molecules) were observed to penetrate into the hydrophobic core of the bilayer region, dragged in via exposed Arg and Lys sidechains on the surface of PorB (Fig. 3). This deformation was evaluated by measuring the headgroup phosphate-phosphate distance between opposing leaflets (Supplementary Information). This revealed that the bilayer thinned from a bulk membrane value of ~4 nm to ~1–2 nm in the immediate vicinity of the protein. Such extreme deformation has been previously observed in simulations of e.g. the highly-charged voltage-sensor domain [42–44].

In contrast with the original model, significant penetration of lipid headgroups and water was *not* observed in the modified model, although there was some "pinching" of the bilayer (to around ~3 nm for the phosphate-phosphate distance) in the vicinity of the pentamer. These differences arise from the rotation of H1 in the modified model, which serves to lengthen the protein and reduce the number of polar/charged residues exposed to the hydrophobic region of the membrane, providing a better match with the hydrophobic region of the phospholipid bilayer (Fig. 3). In particular, the charged Lys34 residues interact with the zwitterionic lipid headgroups, while Arg60 interacts with either residue Glu19 or Glu20 in the loop connecting H1 and H2 of the adjacent subunit. The Arg/Glu interaction, which occurs between adjacent subunits, is facilitated by the spontaneous rotation of H1 observed in our simulations of the monomer. As a consequence of the Lys–lipid headgroup and Arg–Glu interactions, none of the charged residues in the modified model are exposed to the hydrophobic region of the lipid bilayer. The observed "pinching" of the lipid bilayer around the modified model occurs as the bilayer adjusts its width to maximize favourable contacts with the protein and to avoid hydrophobic mismatch. Such local adjustments in phospholipid structure have been reported from extended coarse-grain simulations around other bacterial OMPs [45].

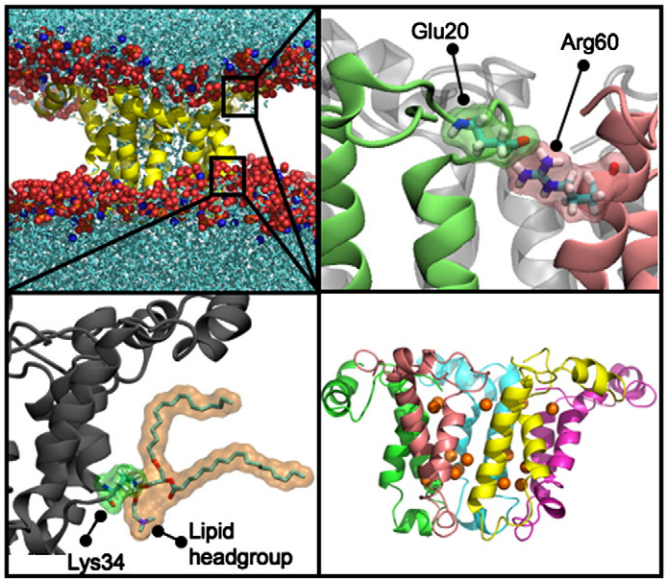

Fig. 3. Final snapshot after a 30 ns atomistic simulation of the modified pentameric model. Top left: the lipid headgroups are shown in blue and red/orange spacefilling format, water molecules are shown as cyan sticks and the protein is shown in yellow cartoon format. Top right: a close-up view showing interaction of Glu20 with Arg60 of the contiguous subunit. The protein is shown in light grey cartoon format with the two interacting subunits in green and pink. Glu20 and Arg60 are shown in stick format. Bottom left: a close-up view showing the interaction of Lys34 with lipid headgroups. The protein is shown in grey cartoon format and the lipid is shown in stick and semitransparent surface format. Bottom right: side view of the protein. Each subunit is shown in a different color. Ca^{2+} ions are shown in orange.

3.3. Extent of membrane insertion of the two models

The coarse-grained (CG) simulation protocol (see Methods section) employed ensures the formation of a self-assembled lipid bilayer. Such self-assembly simulations are useful for extracting unbiased information regarding the location and orientation of membrane proteins within lipid bilayers [36,37,45]. Self-assembly simulations of both the original and our modified PorB model in pure POPC, pure DLPC, and three different mixtures of POPC and DLPC lipids were performed. Five independent replicas of each simulation were performed to improve conformational sampling, resulting in a total of fifty sets of 5 μs trajectories. The final system configurations revealed that, as expected for a homo-oligomer, both models were orientated such that their principal axes were orthogonal to the bilayer plane, whilst the protein tilt angle did not deviate by more than ~3° during any of the simulations. On the other hand, substantial differences were observed in the context of depth of insertion. In the modified model, the orientation of H1 served to lengthen the outer surface of the protein such that it matched up well with the core of the bilayer. In the case of the original model, it appears that the protein structure is too short to fit well in any of the bilayers, regardless of their thickness. The mean distance was calculated between the membrane phosphate groups of each leaflet and the center of mass of Cys64 or Phe38 for the five subunits, which correspond respectively to the residues lying at the pivot between helix H1 and the rest of the protein, and the phe38 and trp39 residues of the H3 helices that define the hydrophobic rim on the intracellular side of the protein (Fig. 1). This was evaluated for the last 100 ns of the 50 simulations, and the results were averaged for the 10 sets of 5 replicas simulations. For both leaflets in DLPC bilayer, which has an average thickness of 3.4 nm—close to that of the mycobacterial membrane—these protein regions were fully embedded within the membrane core for the modified model. In comparison, for the original model, these regions of the protein were shifted by ~1 nm out of each leaflet, i.e. the model inserted incompletely into the membrane. As the concentration of POPC and hence bilayer width increased, the degree of insertion of the modified model gradually reduced, but in comparison, the two rims of the original model remained at least 0.5 nm further displaced from either leaflet in all membrane compositions (Supplementary Information). The shorter hydrophobic width of the original model and its displacement towards the outer leaflet led to the formation of a "semi-pore" by the severely deformed lipids of the opposite leaflet (Fig. 4). It should be noted that in this set of 50 simulations, the distribution of DLPC and POPC lipids was fairly even between leaflets and also as a function of distance to the protein. A 16 μs long trajectory of a significantly larger simulation box at equimolar DLPC/POPC concentration was obtained for the original model, from which this observation was confirmed (Supplementary Information). As our simulations suggest that the preferred conformation of the PorB pentamer in a

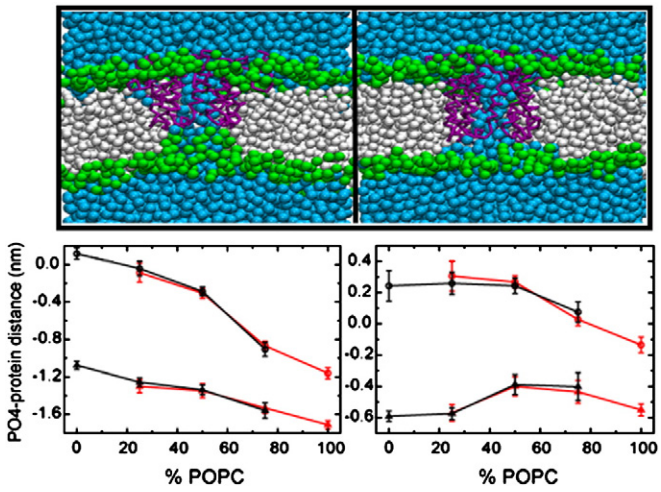

Fig. 4. Top left: side view of the final conformation after 5 μs of coarse grained MD simulation for the porB pentameric original model. Top right: idem for the modified model. The snapshots correspond to one of the five replicas performed for this structure in pure POPC bilayers. Protein backbone atoms are shown in magenta. Lipid heads, lipid tails and water atoms are represented in green, grey and blue spheres, respectively. Bottom left: distances between the average of the PO4 beads of the POPC (red) or DLPC (black) lipids in the outer leaflet and the c.o.m. of the cys64 residues for the original (triangles) and the modified (circles) models. Bottom right: idem between the lipids in the inner leaflet and the phe38 residues of the two PorB structures.

membrane environment is likely to be that adopted by the modified model, we now focus our analyses on this model.

3.4. Protein–lipid interactions

The interactions of a membrane protein with its local environment may help to maintain its structural integrity, facilitate its functional role and mediate its interactions with surrounding proteins. Thus, it is important to gain a molecular-level understanding of these interactions. We have analysed our coarse grained PorB pentamer simulations to identify key areas on the protein that have a high propensity to interact with (a) lipid headgroups and (b) lipid tails (Fig. 5). We find that these interactions have a marked dependency on the type of phospholipids in which the protein is embedded. In general, the lipid tails interact mainly with the transmembrane portion of the outer surface of the protein, with few interactions with the external "rim" of the pore. Unexpectedly, the rim on the intracellular side of the protein makes a significant number of contacts with lipid tail particles. This is due to the partial hydrophobic nature of H3 which makes it stable in the interfacial region between lipid headgroups and tails. In contrast to the general behaviour of the lipid tails, the lipid headgroups have a higher propensity to interact with the residues near both rims. This preferential headgroup interaction with the rims of the pore is most marked in the simulations of the PorB pentamer in POPC lipids. In particular, residues gly16–glu20 (loop 1), phe38 and phe43 (H3) and arg60 (H4) have a high propensity to interact with lipid headgroup articles; these residues together contribute 24.8% of the total number of headgroup-protein interactions. Similar interaction of aromatic residues with lipid headgroups has previously been reported for the traditional β-barrel porins found in Gram-negative bacteria and is thought to anchor the protein in a favourable orientation in the membrane [39,45–47]. As the DLPC (shorter tails) content is increased, the headgroup interactions are spread over a wider range of residues: with residues ala15–glu19 (H1-loop 1), lys34 (H2), gln42 (H3), and ile46, trp49 and arg60 (H4) all participating in these interactions. The shortening of the tails brings the headgroups into closer contact with more of the residues that are mostly, only in contact with the tails in pure POPC. Thus, in our simulations the lipid–protein contacts most closely resemble the patterns reported from comparable simulations of membrane proteins when PorB is in a pure POPC bilayer.

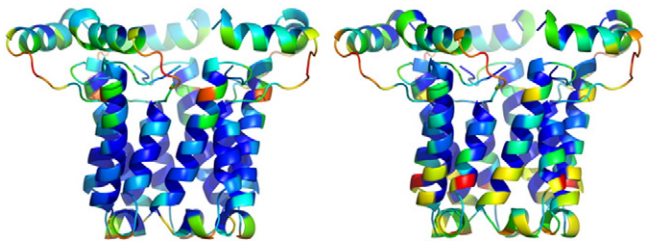

Fig. 5. Structure of the PorB modified model colored with a blue-red gradient as a function of the number of lipid head particles in a POPC (left) and DLPC (right) bilayer.

3.5. Lipid mobility

We have also analysed the mobility of the lipids surrounding the protein. To characterize the lipids in terms of their distance from the protein, we initially calculated the average value and the variance of the minimum distance of each individual lipid to the protein over 1 μs for the five lipid concentrations simulated; 100%, 75%, 50%, 25% and 0% POPC in POPC/DLPC mixtures. Only the particle representing the phosphate moiety of the lipid headgroups (PO4) was used for the distance measurements and all subsequent calculations. The average diffusion coefficient for each individual lipid was calculated from the same trajectories (note that for comparison to atomistic simulation

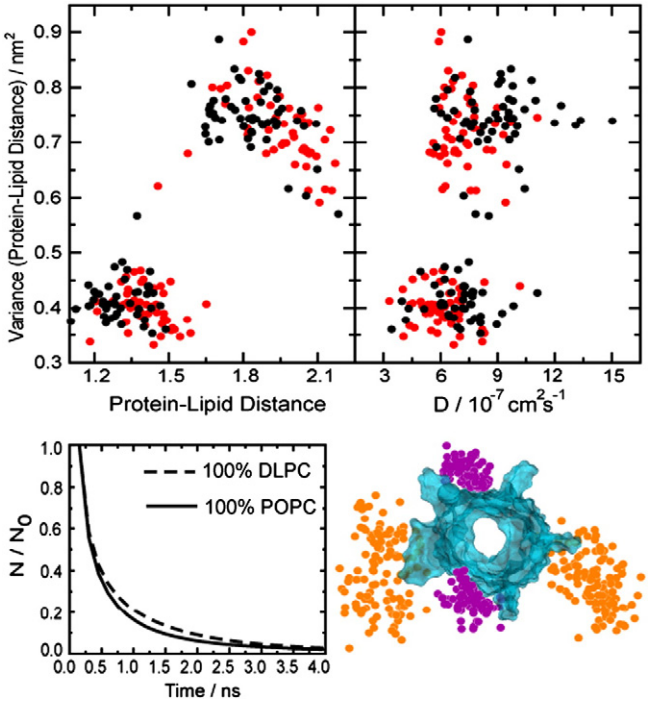

Fig. 6. Top: variance of the protein–lipid distance average during the trajectory as a function of the protein–lipid distance (left) and as a function of the diffusion constant (right). Black and red spots represent DLPC and POPC molecules, respectively. Bottom: decay functions for the protein–lipid contacts corresponding to the trajectories with pure POPC (solid line) and pure DLPC (dashed line). N is the number of protein–lipid contacts which stands at least for a given time and N_0 is the maximum number of contacts at the beginning of the simulation. The calculations are based on the average of all the lipids of each trajectory over 1 μs of simulation time. The image represents the different positions of lipids from **Gp** (magenta), from **Gm** (orange) and the protein (cyan), at different times along the trajectory.

results a conversion factor of 0.25 for the diffusion coefficients should be employed [34]). As shown in Fig. 6 the lipids can be divided in two groups based on the variance of the minimum distance to the protein. The lipids in the group with lower variance (termed **Gp** from here on) are, on average, significantly closer to the protein and also exhibit lower diffusion coefficients. This group consists of 92–100 lipids. The second group of lipids will be termed **Gm**, these are further away from the protein and have higher diffusion coefficients compared to lipids in the **Gp** group. Fig. 6 shows representative results for the systems with equimolar concentration of POPC and DLPC lipids. Encouragingly, similar patterns of lower diffusion rates of "annular" lipids have previously been reported for membrane proteins [39,45–47]. Comparison of the diffusion rates of the two lipid types, DLPC and POPC revealed that POPC has a lower diffusion rate than DLPC, which is not unexpected as POPC is a bulkier molecule (Supplementary Information). In general, the diffusion values calculated from our simulations compare well to those previously reported for lipids from coarse-grain simulations [34]. It is important to note that the diffusion coefficients of **Gp** lipids reported here do not correspond to lipids bound to the protein throughout the trajectories, but to the average diffusion coefficients of lipids which spent a significant part of the trajectory close to the protein. This means that the difference in the diffusion coefficients between protein-bound and protein-unbound lipids is higher, as expected [48]. The diffusion coefficient of bound lipids was estimated to be about 0.17 $cm^2\ s^{-1}$ by selecting trajectory segments for which particular lipids remained at $\leq$ 0.8 nm from the protein. Visual inspection of the trajectories revealed that the **Gp** lipids while being on average closer to the protein, did not in general, remain "bound" to any particular protein residues for significant lengths of time (Fig. 6). We observed the same lipids interacting with different regions of the protein. To quantify this observation, we calculated the mean lifetime of the lipid–protein interactions. The decay functions corresponding to the protein–lipid interactions (where interaction is defined as protein–lipid distance of $\leq$ 0.8 nm) were determined. These revealed that the mean lifetime of lipid–protein interactions is about 0.5 ns for both DLPC and POPC molecules. Thus, while the lipids in the **Gp** group remain in the general vicinity of the protein, each instance of lipid–protein distance of $\leq$ 0.8 nm has a lifetime of only ~0.5 ns. The maximum amount of time that any lipid spent at less than 0.8 nm from any protein atom was about 30% of the total simulation time. Encouragingly, the behaviour of the PorB model with respect to lipids is similar to that reported for a homology model of a membrane protein [39] and also membrane proteins for which high resolution x-ray structures are known [46].

4. Discussion

The X-ray structure of the PorB monomer from *C. glutamicum,* and a model of the functional protein proposed to be a pentamer were recently reported. The present study describes simulations that predict a spontaneous conformational rearrangement of the protein in response to the phospholipid bilayer in which it is embedded, thus demonstrating a remarkable ability of this protein to alter its conformation to adapt to the local environment.

Simulations of the PorB monomer revealed that the secondary structure of the four helical regions H1–H4 was retained. While helices H2 and H4 showed little conformational fluctuation, H1 was observed to undergo spontaneous rotation around the Cys5–Cys64 disulphide bridge, exposing some residues initially buried in a hydrophobic pocket between H1, H2 and H4, to the non-polar phase. A model of the pentamer was built from the modified monomer conformation. This model retained its secondary structure over 30 ns of MD simulation. The Ca^{2+} ions included in the original model remained within the pore throughout, and provided interactions key to the stability of the pentamer.

Two important structural consequences of the rotation of the H1 helix became apparent during the simulations of the pentamer. Firstly, the protein became slightly longer due to H1 rotating in the direction of the extracellular mouth of the porin. This enabled Lys34 to interact with the local zwitterionic lipid headgroups rather than being exposed to the lipid tails. Secondly, rotation of the helix exposed Glu19 and Glu20, such that the sidechain of one of these residues now interacted with and hence "neutralized" lipid-exposed Arg60 in H4. Furthermore, as the interaction of Arg60 and Glu19/20 occurred between neighboring subunits, it not only served to neutralize the oppositely charged sidechains, but also provided a favorable electrostatic interaction that contributed to the overall stability of the pentameric unit. The rearrangement of H1, and consequent dynamics of Arg60 and Lys34, had an effect on the interaction of the protein with its local lipid environment. The modified model of the PorB pentamer did not distort the phospholipid bilayer beyond some thinning in the vicinity of the protein. In stark contrast, simulations of the original pentamer revealed water molecules and lipid headgroup penetrating into the hydrophobic region of the phospholipids bilayer to interact with the two basic residues.

Given the paucity of structural data regarding both the proteins and the membrane composition of Corynebacteria it is imperative to extract the maximum information from the data that is available. We characterized the interaction of the modified model with the surrounded lipids, and measured the effect these interactions had on the mobility of the lipids. Encouragingly we observe similar patterns in the lipid–protein contacts to those reported for other membrane proteins. In POPC the lipid headgroups form contacts with two distinct bands of residues on the surface of the protein. In the shorter DLPC lipids, these bands are less distinct. Our calculations reveal that the diffusion rates of lipids that have a propensity to interact with the protein are about two orders of magnitude lower than those that can be considered "bulk" lipids. In general, we find that lipids do not remain bound to any particular site on the protein but sample various regions on the surface of the protein.

Overall, our simulations together with the X-ray structure reported by Ziegler et al. suggest that this highly unusual porin is able to undergo conformational changes to adapt to its local environment. We describe a model of PorB that arises as a result of spontaneous conformational rearrangement of the monomer determined by X-ray studies. The model pentamer is well suited to a phospholipid bilayer and exhibits lipid–protein interactions similar to those reported for other membrane proteins. It is perhaps useful to reflect on some limitations of the current study; given the paucity of information regarding the *C. glutamicum* membrane, it is not possible for us to perform simulations in a model membrane that accurately reflects the natural environment of PorB. As molecular details of such membranes become available, it will be interesting to simulate PorB in more complex models of lipid/mycolic acid structures. However, while little is known about the architecture and composition of the *C. glutamicum* outer membrane, it is generally thought that the cell walls of Corynebacteria have a heterogeneous structure that can vary in its phospholipid/mycolic acid content. It seems reasonable that this heterogeneity of the membrane structure would require the porins residing within it to have sufficient flexibility in their architecture to respond to the changing environment. As the β-barrel topology of traditional porins from Gram-negative bacteria allows little conformational flexibility, we tentatively suggest that the α-helical architecture of PorB is necessary to afford this porin the required flexibility to adapt its conformation to its local environment.

Acknowledgments

We thank G. Schulz for providing coordinates of the original model and insightful discussions. We also thank J.W. Essex, and M.S.P. Sansom for helpful discussions. Á.P is an Isidro Parga Pondal fellow (Xunta de Galicia) funded by a José Castillejo grant (Ministerio de

Educación y Ciencia del Gobierno Español) to participate in this project. S.K is an RCUK fellow. We are grateful to the "Centro de Supercomputación de Galicia" (CESGA) for computing time.

Appendix A. Supplementary data

Supplementary data to this article can be found online at doi:10.1016/j.bbamem.2011.02.015.

References

[1] S. Khalid, P.J. Bond, T. Carpenter, M.S.P. Sansom, OmpA: gating and dynamics via molecular dynamics simulations, Biochim. Biophys. Acta Biomembr. 1778 (2008) 1871–1880.
[2] G.E. Schulz, The structure of bacterial outer membrane proteins, Biochim. Biophys. Acta Biomembr. 1565 (2002) 308–317.
[3] P.J. Bond, M.S.P. Sansom, The simulation approach to bacterial outer membrane proteins (Review), Mol. Membr. Biol. 21 (2004) 151–161.
[4] V. Puech, M. Chami, A. Lemassu, M.A. Laneelle, B. Schiffler, P. Gounon, N. Bayan, R. Benz, M. Daffe, Structure of the cell envelope of corynebacteria: importance of the non-covalently bound lipids in the formation of the cell wall permeability barrier and fracture plane, Microbiology 147 (2001) 1365–1382.
[5] B. Blombach, G.M. Seibold, Carbohydrate metabolism in *Corynebacterium glutamicum* and applications for the metabolic engineering of l-lysine production strains, Appl. Microbiol. Biotechnol. 86 (2010) 1313–1322.
[6] B. Zuber, M. Chami, C. Houssin, J. Dubochet, G. Griffiths, M. Daffe, Direct visualization of the outer membrane of mycobacteria and corynebacteria in their native state, J. Bacteriol. 190 (2008) 5672–5680.
[7] K. Ziegler, R. Benz, G.E. Schulz, A putative alpha-helical porin from *Corynebacterium glutamicum*, J. Mol. Biol. 379 (2008) 482–491.
[8] E. Barth, M.A. Barcelo, C. Klackta, R. Benz, Reconstitution experiments and gene deletions reveal the existence of two-component major cell wall channels in the genus *Corynebacterium*, J. Bacteriol. 192 (2010) 786–800.
[9] N. Costa-Riu, A. Burkovski, R. Kramer, R. Benz, PorA represents the major cell wall channel of the gram-positive bacterium *Corynebacterium glutamicum*, J. Bacteriol. 185 (2003) 4779–4786.
[10] N. Costa-Riu, E. Maier, A. Burkovski, R. Kramer, F. Lottspeich, R. Benz, Identification of an anion-specific channel in the cell wall of the Gram-positive bacterium *Corynebacterium glutamicum*, Mol. Microbiol. 50 (2003) 1295–1308.
[11] M. Mahfoud, S. Sukumaran, P. Hülsmann, K. Grieger, M. Niederweis, Topology of the porin MspA in the outer membrane of *Mycobacterium smegmatis*, J. Biol. Chem. 281 (2006) 5908–5915.
[12] W. Hu, K.C. Lee, T.A. Cross, Tryptophans in membrane proteins: indole ring orientations and functional implications in the gramicidin channel, Biochemistry 32 (1993) 7035–7047.
[13] A.C.V. Johansson, E. Lindahl, The role of lipid composition for insertion and stabilization of amino acids in membranes, J. Chem. Phys. 130 (2009) 8.
[14] N. Chakrabarti, C. Neale, J. Payandeh, E.F. Pai, R. Pomes, An iris-like mechanism of pore dilation in the CorA magnesium transport system, Biophys. J. 98 (2010) 784–792.
[15] E. Lindahl, O. Edholm, Mesoscopic undulations and thickness fluctuations in lipid bilayers from molecular dynamics simulations, Biophys. J. 79 (2000) 426–433.
[16] O. Berger, O. Edholm, F. Jahnig, Molecular dynamics simulations of a fluid bilayer of dipalmitoylphosphatidylcholine at full hydration, constant pressure, and constant temperature, Biophys. J. 72 (1997) 2002–2013.
[17] G.A. Kaminski, R.A. Friesner, J. Tirado-Rives, W.L. Jorgensen, Evaluation and reparametrization of the OPLS-AA force field for proteins via comparison with accurate quantum chemical calculations on peptides, J. Phys. Chem. B 105 (2001) 6474–6487.
[18] W.L. Jorgensen, D.S. Maxwell, J. TiradoRives, Development and testing of the OPLS all-atom force field on conformational energetics and properties of organic liquids, J. Am. Chem. Soc. 118 (1996) 11225–11236.
[19] H.J.C. Berendsen, J.P.M. Postma, W.F. van Gunsteren, J. Hermans, Interaction models for water in relation to protein hydration, in: B. Pullman (Ed.), Intermolecular forces, D. Reidel Publishing Company, 1981, pp. 331–342.
[20] S. Nosé, M.L. Klein, Constant pressure molecular dynamics for molecular systems, Mol. Phys. 50 (1983) 1055–1076.
[21] M. Parrinello, A. Rahman, Polymorphic transitions in single crystals: a new molecular dynamics method, J. Appl. Phys. 52 (1981) 7182–7190.
[22] W.G. Hoover, Canonical dynamics: equilibrium phase-space distributions, Phys. Rev. A 31 (1985) 1695.
[23] S.I. Nosé, A molecular dynamics method for simulations in the canonical ensemble, Mol. Phys. 52 (1984) 255–268.
[24] U. Essmann, L. Perera, M.L. Berkowitz, T. Darden, H. Lee, L.G. Pedersen, A smooth particle mesh Ewald method, J. Chem. Phys. 103 (1995) 8577–8593.
[25] T. Darden, D. York, L. Pedersen, Particle mesh Ewald: an N.log(N) method for Ewald sums in large systems, J. Chem. Phys. 98 (1993) 10089–10092.
[26] I.C. Yeh, M.L. Berkowitz, Ewald summation for systems with slab geometry, J. Chem. Phys. 111 (1999) 3155–3162.
[27] R.W. Hockney, J.W. Eastwood, Computer Simulation Using Particles, Adam Hilger, New York and Bristol, 1988.
[28] S. Miyamoto, P.A. Kollman, Settle: an analytical version of the SHAKE and RATTLE algorithm for rigid water models, J. Comput. Chem. 13 (1992) 952–962.
[29] B. Hess, H. Bekker, H.J.C. Berendsen, J. Fraaije, LINCS: a linear constraint solver for molecular simulations, J. Comput. Chem. 18 (1997) 1463–1472.
[30] H.J.C. Berendsen, D. van der Spoel, R. van Drunen, GROMACS: a message-passing parallel molecular dynamics implementation, Comput. Phys. Commun. 91 (1995) 43–56.
[31] B. Hess, C. Kutzner, D. van der Spoel, E. Lindahl, GROMACS 4: algorithms for highly efficient, load-balanced, and scalable molecular simulation, J. Chem. Theory Comput. 4 (2008) 435–447.
[32] D. Van der Spoel, E. Lindahl, B. Hess, G. Groenhof, A.E. Mark, H.J.C. Berendsen, GROMACS: fast, flexible, and free, J. Comput. Chem. 26 (2005) 1701–1718.
[33] E. Lindahl, B. Hess, D. van der Spoel, GROMACS 3.0: a package for molecular simulation and trajectory analysis, J. Mol. Model. 7 (2001) 306–317.
[34] S.J. Marrink, A.H. de Vries, A.E. Mark, Coarse grained model for semiquantitative lipid simulations, J. Phys. Chem. B 108 (2004) 750–760.
[35] P.J. Bond, C.L. Wee, M.S.P. Sansom, Coarse-grained molecular dynamics simulations of the energetics of helix insertion into a lipid bilayer, Biochemistry 47 (2008) 11321–11331.
[36] P.J. Bond, J. Holyoake, A. Ivetac, S. Khalid, M.S.P. Sansom, Coarse-grained molecular dynamics simulations of membrane proteins and peptides, J. Struct. Biol. 157 (2007) 593–605.
[37] P.J. Bond, M.S.P. Sansom, Insertion and assembly of membrane proteins via simulation, J. Am. Chem. Soc. 128 (2006) 2697–2704.
[38] H.J.C. Berendsen, J.P.M. Postma, W.F.V. Gunsteren, A. DiNola, J.R. Haak, Molecular dynamics with coupling to an external bath, J. Chem. Phys. 81 (1984) 3684–3690.
[39] S. Khalid, P.J. Bond, S.S. Deol, M.S.P. Sansom, Modeling and simulations of a bacterial outer membrane protein: OprF from *Pseudomonas aeruginosa*, Proteins 63 (2006) 6–15.
[40] S. Khalid, M.S.P. Sansom, Molecular dynamics simulations of a bacterial autotransporter: NalP from *Neisseria meningitidis*, Mol. Membr. Biol. 23 (2006) 499–508.
[41] O.S. Smart, J.G. Neduvelil, X. Wang, B.A. Wallace, M.S.P. Sansom, HOLE: a program for the analysis of the pore dimensions of ion channel structural models, J. Mol. Graph. 14 (1996) 354–360.
[42] J.A. Freites, D.J. Tobias, G. von Heijne, S.H. White, Interface connections of a transmembrane voltage sensor, Proc. Natl Acad. Sci. USA 102 (2005) 15059–15064.
[43] P.J. Bond, M.S.P. Sansom, Bilayer deformation by the Kv channel voltage sensor domain revealed by self-assembly simulations, Proc. Natl Acad. Sci. USA 104 (2007) 2631–2636.
[44] Z.A. Sands, M.S.P. Sansom, How does a voltage sensor interact with a lipid bilayer? Simulations of a potassium channel domain, Structure 15 (2007) 235–244.
[45] K.A. Scott, P.J. Bond, A. Ivetac, A.P. Chetwynd, S. Khalid, M.S.P. Sansom, Coarse-grained MD simulations of membrane protein-bilayer self-assembly, Structure 16 (2008) 621–630.
[46] S. Haider, S. Khalid, S.J. Tucker, F.M. Ashcroft, M.S.P. Sansom, Molecular dynamics simulations of inwardly rectifying (Kir) potassium channels: a comparative study, Biochemistry 46 (2007) 3643–3652.
[47] S.S. Deol, P.J. Bond, C. Domene, M.S.P. Sansom, Lipid–protein interactions of integral membrane proteins: a comparative simulation study, Biophys. J. 87 (2004) 3737–3749.
[48] P.S. Niemela, M.S. Miettinen, L. Monticelli, H. Hammaren, P. Bjelkmar, T. Murtola, E. Lindahl, I. Vattulainen, Membrane proteins diffuse as dynamic complexes with lipids, J. Am. Chem. Soc. 132 (2010) 7574–7575.